Acta Pharmaceutica Sinica B 2021;11(9):2835–2849

Chinese Pharmaceutical Association
Institute of Materia Medica, Chinese Academy of Medical Sciences

Acta Pharmaceutica Sinica B

www.elsevier.com/locate/apsb
www.sciencedirect.com

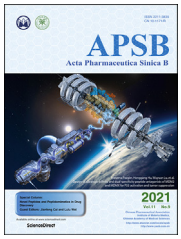

ORIGINAL ARTICLE

Tryptophan 2,3-dioxygenase 2 controls M2 macrophages polarization to promote esophageal squamous cell carcinoma progression *via* AKT/GSK3β/IL-8 signaling pathway

Yumiao Zhao[a], Jiaxin Sun[a], Yin Li[b], Xiuman Zhou[a], Wenjie Zhai[a], Yahong Wu[a], Guanyu Chen[c], Shanshan Gou[a], Xinghua Sui[c], Wenshan Zhao[a], Lu Qiu[a], Yongjie Yao[a], Yixuan Sun[a], Chunxia Chen[a], Yuanming Qi[a,*], Yanfeng Gao[a,c,*]

[a]*School of Life Sciences, Zhengzhou University, Zhengzhou 450001, China*
[b]*Thoracic Surgery Department, National Cancer Center/National Clinical Research Center for Cancer/Cancer Hospital, Chinese Academy of Medical Sciences and Peking Union Medical College, Beijing 100021, China*
[c]*School of Pharmaceutical Sciences (Shenzhen), Sun Yat-sen University, Shenzhen 518107, China*

Received 4 December 2020; received in revised form 29 January 2021; accepted 10 February 2021

KEY WORDS

Tryptophan 2,3-dioxygenase 2;
M2 macrophage;
Esophageal squamous cell carcinoma;
IL-8;
KYN

Abstract Tryptophan 2,3-dioxygnease 2 (TDO2) is specific for metabolizing tryptophan to kynurenine (KYN), which plays a critical role in mediating immune escape of cancer. Although accumulating evidence demonstrates that TDO2 overexpression is implicated in the development and progression of multiple cancers, its tumor-promoting role in esophageal squamous cell carcinoma (ESCC) remains unclear. Here, we observed that TDO2 was overexpressed in ESCC tissues and correlated significantly with lymph node metastasis, advanced clinical stage, and unfavorable prognosis. Functional experiments showed that TDO2 promoted tumor cell proliferation, migration, and colony formation, which could be prevented by inhibition of TDO2 and aryl hydrocarbon receptor (AHR). Further experimentation demonstrated that TDO2 could promote the tumor growth of KYSE150 tumor-bearing model, tumor burden of C57BL/6 mice with ESCC induced by 4-NQO, enhance the expression of phosphorylated AKT, with subsequent phosphorylation of GSK3β, and polarization of M2 macrophages by upregulating interleukin-8 (IL-8) to accelerate tumor progression in the tumor microenvironment (TME). Collectively, our results discovered that TDO2 could upregulate IL-8 through AKT/GSK3β to direct the polarization of M2 macrophages in ESCC, and suggested that TDO2 could represent as

*Corresponding authors. Tel.: +86 371 67783235.
E-mail addresses: qym@zzu.edu.cn (Yuanming Qi), gaoyf29@mail.sysu.edu.cn (Yanfeng Gao).

Peer review under responsibility of Chinese Pharmaceutical Association and Institute of Materia Medica, Chinese Academy of Medical Sciences.

https://doi.org/10.1016/j.apsb.2021.03.009

an attractive therapeutic target and prognostic marker to ESCC.

1. Introduction

Esophageal squamous cell carcinoma (ESCC) is the most common histological subtype of esophageal cancer, and approximately 90% of patients with esophageal cancer in China is ESCC[1,2]. The major clinical used drugs for ESCC treatment are chemotherapeutic agents, which can hardly prolong the overall survival of the patients. Although targeted therapy as gefitinib (an EGFR-TKI) and dovitinib (an FGFR inhibitor), and immunotherapy as PD-1/PD-L1 blockade have achieved great success in management of multiple malignancies including non-small-cell lung cancer (NSCLC) and melanoma, only a small subset of patients with ESCC have acquired clinical benefits[3−6]. Therefore, it is of great importance to discover novel therapeutic targets and strategies for ESCC beyond chemotherapy.

Recently, it was reported that the metabolism of the essential amino acid tryptophan (TRP) through the kynurenine (KYN) pathway has been correlated with the prognosis of several tumor types including colon cancer, breast cancer, and melanoma[7−11]. Tryptophan can be catalyzed into KYN mainly by indoleamine-2,3-dioxygenase 1 (IDO1) and tryptophan-2,3-dioxygenase 2 (TDO2), and KYN could thus suppress the antitumor immune responses directly or indirectly regulated by the AHR[12,13]. AHR is a member of Per-ARNT-Sim (PAS) superfamily of transcription factors best known for its activation by xenobiotics such as KYN[12,14]. Increased AHR activity modulated by TDO2 has been found to improve cancer cells proliferation, migration and invasion in several cancer types, which leads to the transcription of AHR target genes[11,15]. Therefore, IDO1 and TDO2 have been considered as promising antitumor targets. IDO1 was reported to correlate with the clinical outcome and immune status of the tumor patients[16−18]. Therefore, numerous efforts have focused on the development of IDO1 inhibitors, but the clinical trials have not demonstrated significant clinical benefits[19]. The most advanced IDO1 inhibitor epacadostat failed to show improved efficacy of anti-PD-1 (Keytruda) in phase III clinical trial of melanoma[20]. More recently, TDO2 has been shown to promote tumor growth in a similar fashion compared with IDO1. Although IDO1 and TDO2 were both upregulated in ESCC tissues by microarray and qRT-PCR, there was a much higher difference to the expression of TDO2 between ESCC tissues and paired peritumor tissues than that of IDO1 (Supporting Information Fig. S1A−S1D). These results prompted us to investigate the factors affecting the tumorigenicity of TDO2. Although the clinical relevance of TDO2 upregulation in ESCC has been reported, the underlying mechanism for regulating ESCC progression by TDO2 has not been elucidated yet.

The tumor microenvironment (TME) plays a key role in cancer development and metastasis. Among immune cell infiltrated in TME, macrophages are considered composed with a tumor-suppressive (M1) phenotype and a tumor-supportive (M2) phenotype. The accumulation of M2 macrophages has been associated with poor clinical prognosis and described as a suppressor of inflammatory responses in solid tumors including ESCC[21−23]. The tumor cells could recruit macrophages into the tumor tissues and promote the polarization of M2 macrophages, which in turn further facilitate the malignant progression of the tumor. IDO1 may contribute to the predominance of M2 macrophage in several diseases[24−26]. However, whether TDO2 could regulate the recruitment and polarization of macrophages in TME remains largely unknown.

Here, we discovered that the mRNA and protein expression of TDO2 in ESCC tissues were higher than that in normal tissues, and the high expression of TDO2 protein in ESCC tissues indicated the poor prognosis. *In vitro* assays of MTT, wound heading, Transwell, and colony formation were subsequently performed, and the results suggested that TDO2 might promote the proliferation and invasion of ESCC by its metabolized product KYN rather than quinolinic acid (QA) or picolinic acid (PA). TDO2 or AHR antagonist significantly reduced tumor burden and the infiltration of M2 macrophages in tumor bearing nude mice lacking intact adaptive immunity, suggesting that TDO2 functions to support tumor growth and skew macrophages toward a M2-polarized phenotype. This was also confirmed in a 4-NQO induced ESCC mouse model. Finally, we discovered that the IL-8 might play a key role in mediating the M2 macrophage polarization by TDO2. These findings demonstrated a novel mechanism of TDO2 in promoting ESCC, and proposed a potential therapeutic target to ESCC treatment.

2. Materials and methods

2.1. Patients and tumor specimens

A total of 159 patients with ESCC underwent esophagectomy between 2010 and 2015 from the Affiliated Cancer Hospital of Zhengzhou University were included in this study (Supporting Information Table S1). All the patients were not treated chemotherapy, radiotherapy, or other therapy before the surgery. The clinicpathologic features were collected, including age, gender, tumor site, differentiation lymph node metastasis, and clinical TNM stage. Ethical consent was approved by the Ethics Committee of Zhengzhou University (ZZU-20180312), Zhengzhou, China.

2.2. Cell culture

ESCC cell lines (KYSE70, KYSE140, KYSE150, KYSE450, EC1, EC109, and EC9706), normal esophagus epithelial Het-1A cell line, and HEK-293T cell line were purchased from Cell Bank Shanghai Institutes for Biological Sciences of Chinese Academy of Sciences, Shanghai, China. HEK-293T cells were cultured in DMEM medium (Gibco, Grand Island, USA), and other cell lines were cultured in RPMI 1640 medium (Gibco), supplemented with 10% fetal bovine serum (FBS, BI, Israel), 100 U/mL penicillin (Solarbio) and 100 μg/mL streptomycin (Solarbio, China). Cells were maintained in a humidified incubator at 37°C in 5% CO_2.

2.3. Reagents

TRP (T8941-25G), KYN (K8625-100MG), QA (P63204-25G), PA (P42800-5G), TDO2 inhibitor 680C91 (SML0287-5MG), and AHR antagonist CH-223191 (C8124-5MG) were purchased from Sigma (USA). AKT inhibitor AZD5363 (S8019), GSK3β inhibitor CHIR-22901 (CT99021), CXCR1/CXCR2 inhibitor reparixin (S8640) were purchased from Selleck (USA). Each was solubilized according to manufacturer's recommendations. The levels of IL-8 in culture supernatants were measured by ELISA technique (Invitrogen, 88-8086-88, USA), following the manufacturer's instructions.

For Western blot analysis, detailed experiments were performed as described previously[27]. Total protein extracted from cell lines were subjected to separation by SDS-PAGE and transferred to PVDF membrane (Millipore, USA). Antibodies against β-actin (Abcam, #AC004), TDO2 (Sango Biotech, #D199153), AKT (Cell Signaling Technology, #4685), phosphorylated AKT (Ser473, Cell Signaling Technology, #4060S), GSK3β (Cell Signaling Technology, #9315), and phosphorylated GSK3β (Ser9, Cell Signaling Technology, #9323) were used. The PVDF membranes were incubated with the primary antibody overnight at 4°C, and subsequently visualized by a Phototope-Horseradish Peroxidase Western Blot Detection Kit.

2.4. RNA isolation and quantitative real-time polymerase chain reaction (qRT-PCR)

Total RNA was isolated from cells or tissue specimens using E.Z.N.A. Total RNA Kit II (Omega, USA) was converted to cDNA using the RevertAid cDNA Synthesis Kit (Thermo Scientific, USA) according to the manufacturer's instructions. qRT-PCR was accomplished using the SYBR-green method on a Roche LightCycler 480 SYBR Green I Master. The primer sequences (Sangon Biotech, China) for RT-PCR and qRT-PCR in this study were listed in Supporting Information Table S2, respectively. GAPDH was used to determine the relative expression of each gene. The data were analyzed by $2^{-\Delta\Delta Ct}$.

2.5. Plasmids and lentiviral transfection

The stable overexpression of TDO2 in KYSE150 and KYSE450 and detailed experiments were performed as described previously[28]. Briefly, full-length TDO2 cDNA (Supporting Information Table S3) extracted from ESCC tumor was amplified by PCR using PrimeSTAR HS DNA Polymerase (TaKaRa, Japan), and subcloned into XhoI and BamHI sites of pLVX-puro vector (Clonetech) to produce lentivirus in HEK-293T. KYSE150 and KYSE450 cells were transfected with concentrated virus using Lipofectamine 2000 (Invitrogen) and then cultured for 48 h, followed by puromycin selection (0.1 mg/mL, Sigma). Cells transfected with empty vector were used as negative control.

2.6. MTT assay

Cell growth rate was assessed by MTT (Sigma) assay. Briefly, cells were seeded in 96-well plates at a density of 2000 cells/well and cultured for 8 h. Then cells were starved in medium without FBS for 12 h prior to the experiments. After every 24 h, cell viability was detected using MTT assay (5 mg/mL) and incubated for 4 h. The absorbance of each well was measured at 490 nm by using a spectrometer (Thermo Scientific, USA). The results are expressed as the mean ± standard error of mean (SEM) of three independent experiments.

2.7. Migration assay

Migration assay was performed using the Transwell chamber migration assay (Corning, MA, USA) without Matrigel according to the manufacturer's protocols. The Transwell assay was performed in a 24-well plate. In brief, cells (1×10^5) were plated on the top chamber in 200 μL serum-free medium. A 600 μL of RPMI 1640 containing 10% FBS was added to the bottom chamber. After incubation for 36 h at 37°C in a 5% CO_2 incubator, the cells migrated through the filters were fixed with methanol and stained with 0.5% crystal violet, and the stained cells were counted in ten random fields under a microscope[29].

For wound healing assay, 2×10^5 cells were plated in a 24-well plate. The cells reached confluence over 95% after incubation for 36 h, and a monolayer of cells was scratched vertically by a 200 μL pipette tip. Cells were then washed with PBS to remove the floating cells. Fresh RPMI 1640 medium without FBS was added, and photos were taken after incubation for 12 h to access cell migration using a light microscope.

2.8. Colony formation assay

KYSE150-Vector, KYSE150-TDO2, KYSE450-Vector, or KYSE450-TDO2 cells were seeded into a 6-well plate with 500 cells/well. After 10 days of culture, the cells were fixed with methanol and stained with 0.5% crystal violet, and then the colonies of cells were counted. The results are expressed as the mean ± SEM of three independent experiments.

2.9. Co-culture of peripheral blood mononuclear cell (PBMC)-derived macrophages and KYSE150 cells

PBMCs from healthy donors were obtained as described previously[30]. To induce macrophage-like cells, PBMCs (1.5×10^7 cells) were cultured in 6-well plates and treated with M-CSF (50 ng/mL, Peprotech) for 6 days. The medium was refreshed every 3 days. In order to induce the M2 macrophages, macrophage-like cells were seeded in the bottom chamber of a 6-well plate and co-cultured with 1.5×10^5 KYSE150-Vector or KYSE150-TDO2 cells for 24 h by inserting with a 0.4-μm pore-size filter (Corning, MA, USA). IL-8 was neutralized with 20 ng/mL of anti-human CXCL8/IL-8 neutralized antibody (R&D systems, Abingdon, UK).

2.10. Xenograft tumor assays

All animal procedures were approved by the Ethics Committee of Zhengzhou University, Zhengzhou, China. To generate the xenograft mice model, 2×10^6 KYSE150-Vector or KYSE150-TDO2 cells were injected subcutaneously into the right flank of 6-week-old female BALB/c nude mice (five or six mice per group). From Day 1 to Day 19 after tumor inoculation, mice received drinking water, oral 680C91 (15 mg/kg, pH = 2.5) every 3 days, or oral CH-223191 (10 mg/kg in corn oil) every 3 days[31–33]. To establish a macrophage depletion model, mice were injected by tail vein with Clophosome®-clodronate liposomes (CCL, neutral, FormuMax) or control neutral liposome (CNL) at an initial dose of 0.1 mL once every 3 days from the day before tumor bearing. Mice in the vector or TDO2 group received tail vein injection of PBS[34]. Reparixin (30 mg/kg) was administered subcutaneously

every 3 days between Days 1 and 18. The control mice received 100 μL of a saline solution. The tumor volumes were measured every 3 days and calculated as length × width × height × 0.5.

2.11. *ESCC tumor model induced by 4-NQO in mice and drug treatments*

Six-week-old female C57BL/6 mice purchased from Vital River Laboratory (Beijing, China) were used in the present study. The 4-NQO (Sigma) was dissolved in the drinking water at 100 μg/mL[35]. All mice received 4-NQO for 16 weeks and then changed to normal drinking water for another 12 weeks (five mice per group); mice were grouped randomly and then treated with normal drinking water, 680C91 (15 mg/kg) or CH-223191 (10 mg/kg in corn oil) every 3 days for 4 weeks. The food and water intake were monitored weekly. Mice dying prior to the end of the experiment were excluded from the analysis. Mice were sacrificed at the end of the experiment, and whole esophagi were opened longitudinally, and macroscopic lesions were observed and analyzed carefully.

2.12. *Expression dataset analysis*

Publicly available databases were used to analyze the TDO2 expression levels in human ESCC and normal tissues. The Cancer Genome Atlas (TCGA) data for variations of TDO2 in ESCC analyzed in this study was accessed from the UCSC Xena browser (http://xena.ucsc.edu). The mRNA expression data was represented by RNA-seq (Illumina HiSeq platform) include RSEM (RNA sequencing by Expectation-Maximization) normalized level 3 data presented in TCGA as of February 29, 2020. RNA-seq data from ESCC and the matched normal tissues were obtained from dataset GSE23400 and GSE20347 in Gene Expression Omnibus (GEO; http://www.ncbi.nlm.nih.gov/geo). ESCC samples in TCGA were divided into low expression group and high expression group according to the mean value of TDO2 expression. Gene enrichment analysis was performed using GSEA software (https://www.broadinstitute.org/gsea/). Gene sets with P values < 0.05 and absolute value of NES > 1 are considered to be significantly enriched.

2.13. *Flow cytometry analysis of macrophages*

After the mice were sacrificed, tissues were homogenized and incubated for 45 min at 37°C in an enzymatic cocktail containing 100 U/mL collagenase IV (Invitrogen, #17104019) and 100 U/mL DNase I (Sigma, #DN25) in an enzymatic digestion buffer containing PBS[28]. Single cell suspension of mouse esophagus and tumor were prepared by gentle mechanical disruption, and stained with antibodies to analyze the M1 and M2 macrophages as following: FITC-conjugated mouse anti-CD45 (30-F11, eBioscience), Percp-Cy5.5-conjugated mouse anti-CD11b (M1/70, eBioscience), eFluor 450-conjugated mouse anti-F4/80 (BM8, eBioscience), APC-conjugated mouse anti-CD11c (N418, eBioscience), and corresponding isotype controls (eBioscience), PE-conjugated anti-mouse CD206 (MMR, Biolegend) and isotype control (Biolegend). The samples were harvested and analyzed with a BD FACSCelesta (BD Bioscience) flow cytometry.

Ex vivo polarized macrophages were also detected by flow cytometry methods. In brief, the freshly isolated cells were washed with PBS, and Fc receptor were blocked with PBS containing 10% rat serum 15 min before staining. 1×10^6 cells were incubated with surface-marker CD163-PE (eBioGHI/61, eBioscience). Equivalent amounts of isotype-mached control antibody (Mouse IgG1 Kappa Isotype Control, P3.6.2.8.1, eBioscience) and unstained cells were included in the experiment as negative and autofluorescence control. All cells were analyzed with a BD FACSCelesta (BD Bioscience) flow cytometry[36].

2.14. *Pharmacological treatment*

AZD5363 (AZD), the inhibitor of AKT, was used to prevent the activation of AKT. Cells were treated with 5 μmol/L AZD5363 in a humidified incubator with 5% CO_2 for different hours at 37 °C.

CHIR-99021 (CHIR), the inhibitor of GSK3β, was used to prevent the activation of GSK3β. Cells were treated with 5 μmol/L CHIR-99021 in a humidified incubator with 5% CO_2 for different hours at 37 °C.

2.15. *Statistical analysis*

For functional analysis, data are presented as mean ± SEM. Paired or unpaired t-test was used to compare gene expression between ESCC tissues and normal tissues, while the comparison of more than two groups was conducted using one-way ANOVA. The cutoff value for TDO2 expression level was stratified using median cut-point. The Pearson χ^2 test analyzed the association between TDO2 expression and clinicopathologic features. Kaplan−Meier analysis was used for survival analysis and the survival difference between subgroups was compared by log-rank test. Correlations between the expressions of two genes were determined using Spearman's correlation test. All statistical analyses were performed using SPSS (version 21.0, SPSS Inc.). A P value < 0.05 was considered statistically significant.

3. Results

3.1. *TDO2 was upregulated and associated with survival of patients in ESCC*

The expression of TDO2 has been previously studied in breast cancer[11], hepatocarcinoma[31], ESCC[37], and glioma[38]. In this study, we found that the expression levels of *TDO2* was also higher in 84 esophageal tumor tissues than peritumor tissues by microarray (Fig. 1A). To verify this, qRT-PCR was performed to examine the expression of *TDO2* in paired ESCC and peritumor tissues. The mRNA expression levels of *TDO2* were significantly higher in 34 pairs of tumor tissues than adjacent peritumor tissues (Fig. 1A). To the existing databases GSE23400 and GSE20347, the expression levels of *TDO2* in ESCC tissues were also higher than adjacent normal tissues (Fig. 1B).

To evaluate the oncogenic function of TDO2, we examined the expression of *TDO2* in an immortalized esophageal epithelial cell line and ESCC cell lines. The results show that the expression level of *TDO2* significantly decreased in KYSE150 and KYSE450 (Fig. S1E). ESCC samples and their corresponding non-tumor tissues were collected to verify the expression of TDO2 by immunohistochemistry (IHC) staining. The potential clinical relevance of TDO2 expression in patients with ESCC was analyzed, and the representative IHC images are shown in Fig. 1C. Interestingly, a large set of peritumor specimens were undetectable for TDO2 protein, while 98.7% of ESCC specimens possessed detectable TDO2 protein levels. Although TDO2 expression was

detected at relative low level in ESCC cell lines, TDO2 was positive in both immune cells and tumor cells (Fig. S1F). Kaplan−Meier survival analysis showed that higher TDO2 expression was associated with decreased patient survival (log-rank test, $P = 0.0294$, Fig. 1D). We also found that the upregulation of TDO2 was significantly correlated with gender ($P = 0.026$), TNM stage ($P = 0.021$), and lymph node metastasis ($P = 0.024$), whereas the level of TDO2 had no significant correlation with age, tumor tissue differentiation level or location (Table 1).

In summary, both mRNA and protein expression levels of TDO2 were markedly up-regulated in ESCC specimens, and TDO2 protein expression was correlated with poor survival of the patients of ESCC, suggesting that the aberrantly overexpression TDO2 may play an important role in promoting ESCC.

3.2. *TDO2-mediated KYN production promotes ESCC cells proliferation and migration via AHR pathway*

To investigate the role of TDO2 in ESCC progression, TDO2-overexpressing sublines from two ESCC cell lines KYSE150 and KYSE450 were established. The expression of TDO2 was determined by qRT-PCR and Western blot (Fig. 2A). The secretion level of KYN was detected by using HPLC, which was higher in TDO2-overexpressing cells in 80 μmol/L TRP medium for 18 h than control cells (Fig. 2B). Even though there was no difference, lower TRP concentrations were measured in the culture of TDO2-overexpressing cells (Supporting Information Fig. S2A). Pairwise comparisons revealed no differences in the concentrations of QA and PA immediately compared to the vector control as shown in Fig. S2B and S2C. We also detected that the secretion level of KYN reduced after TDO2 inhibition (Fig. S2E), where the concentration of TRP increased (Fig. S2D). These findings indicate that increased secretion of KYN instead of QA or PA in TDO2-overexpressing ESCC cells was dependent on TDO2 activity.

Table 1 Correlation analysis between the expression of TDO2 and clinicopathological parameters in ESCC patients.

Variables	All cases	TDO2 expression		P^a
		Low	High	
Total	75	37	38	
Age				0.341
<60	30	16 (53%)	14 (47%)	
≥60	45	21 (47%)	24 (53%)	
Gender				0.026*
Male	51	22 (43%)	29 (57%)	
Female	24	15 (63%)	9 (37%)	
TNM stage				0.021*
I + IIa	31	19 (61%)	12 (39%)	
IIb + III	44	18 (41%)	26 (59%)	
Lymph node metastasis				0.024*
N0	39	23 (59%)	16 (41%)	
N ≥ 1	36	14 (39%)	22 (61%)	
Differentiation				0.383
I	34	18 (53%)	16 (47%)	
II + III	41	19 (46%)	22 (54%)	
Location				0.246
Upper	13	11 (85%)	2 (15%)	
Middle	45	17 (38%)	28 (62%)	
Lower	17	8 (47%)	9 (53%)	

*$P < 0.05$ is compared significant

[a]P values for comparing clinicopathological parameters in TDO2 low-expression group *versus* high-expression group.

The effects of TDO2 on the proliferation, migration and colony formation of overexpressed cell lines were determined. As shown in Fig. 2C, the MTT assay shows that TDO2 significantly enhanced the proliferation of KYSE150 and KYSE450 cells. Stably overexpression of TDO2 in these cells substantially

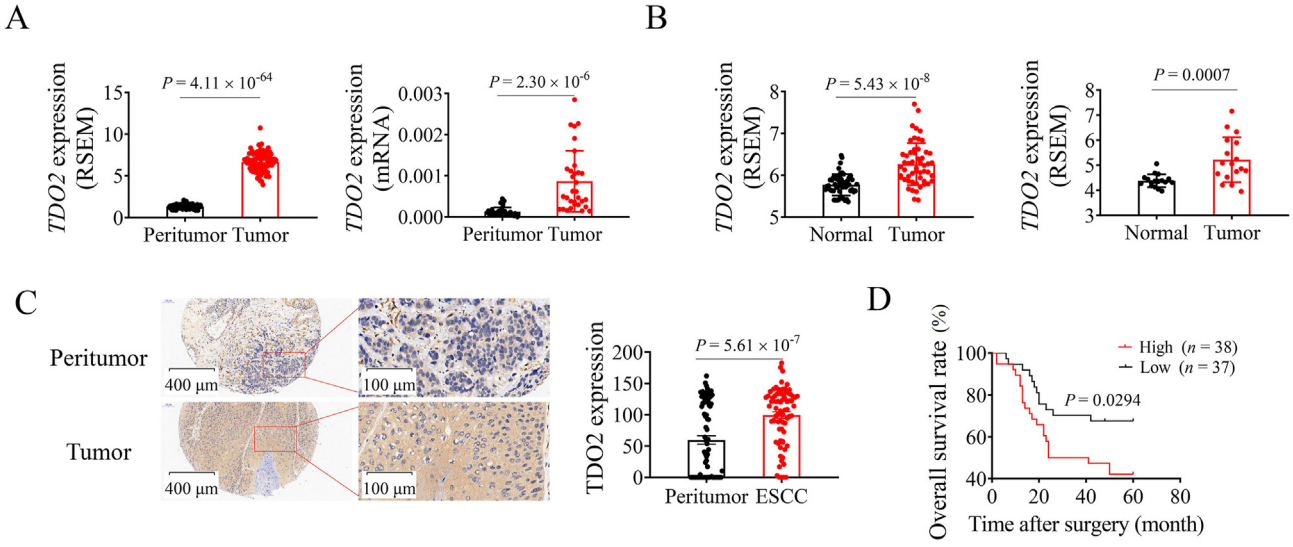

Figure 1 Expression of TDO2 in esophageal tissues and its prognostic value in ESCC patients. (A) Relative mRNA levels of *TDO2* were examined by microarray analysis in 84 paired ESCC patients (left), and by qRT-PCR analysis in 34 paired ESCC patients (right). *GAPDH* was used as reference to normalize the data. The data was analyzed using $2^{-\Delta\Delta Ct}$. (B) Comparison of the mRNA levels of *TDO2* in ESCC from GEO dataset (GSE23400 and GSE20347). Results are displayed as individual points. Paired *t*-test was used to compare the difference. (C) TDO2 protein levels were detected by immunohistochemistry staining in randomly selected ESCC and paired peritumor tissues. (D) Kaplan−Meier survival analysis of overall survival based on high ($n = 38$) and low ($n = 37$) expression of TDO2 by IHC. All data are displayed as mean ± SEM; P values are shown on the graph.

enhanced their migration, as assessed by the wound healing and the Transwell assays (Fig. 2D and E). Furthermore, the colony formation assay yielded a higher number of colonies in TDO2-overexpressing cells than the negative control (Fig. 2F). Together, these data illustrate the importance of TDO2 expression as a driver of neoplastic proliferation, migration and colony formation.

To further verify the tumor-promoting role of TDO2 and AHR in ESCC cells, KYSE150-TDO2 and KYSE450-TDO2 cells were treated with the TDO2 inhibitor 680C91, or the AHR inhibitor CH-223191. Tumor cells were treated with a specific TDO2 inhibitor (680C91) as surrogate to the knockdown of TDO2, which has been reported elsewhere[8]. Both inhibitors significantly decreased the proliferation of cells by MTT assay (Fig. 2C). Additionally, inhibition of TDO2 and AHR significantly reduced the migration and colony formation of KYSE150-TDO2 and KYSE450-TDO2 cells (Fig. 2D–F). The results suggest that inhibition of TDO2 or AHR could reduce TDO2-induced ESCC cells proliferation, migration and colony formation.

KYN is a putative endogenous ligand for AHR, suggesting a potential relationship between TDO2 expression and AHR activation in ESCC cells. We thus sought to determine whether KYN

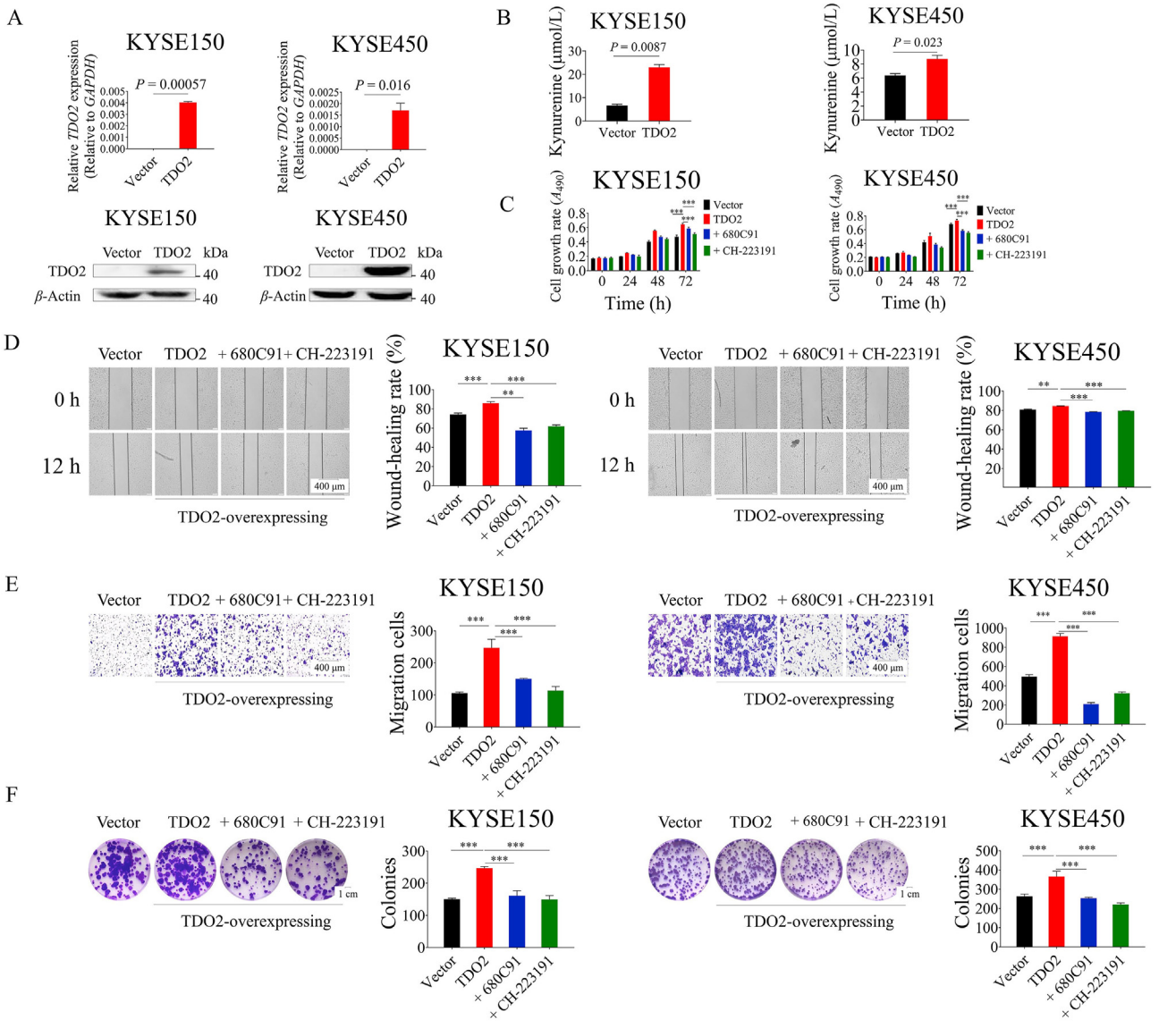

Figure 2 Overexpression of TDO2 plays an important oncogenic role in ESCC cells, and effects of blocking TDO2−AhR pathway on cell proliferation, migration and colony formation. (A) qRT-PCR analysis (upper panel) and Western blot (lower panel) of TDO2 in KYSE150 and KYSE450 cells expressing TDO2 and vector. (B) KYN concentration in the medium of TDO2-overexpressing (TDO2) and control (Vector) ESCC cell lines. (C) Growth rates of vector, TDO2 cells, and with 680C91 or CH-223191 by MTT assay. (D) Wound-healing assay. Representative wound closing cells (12 h) after scratching (0 h) of vector, TDO2 cells with 680C91 or CH-223191 (left, representative pictures; right, bar charts indicating the wound healing rate. Magnification 100 ×). (E) Transwell assays for migration of Vector, TDO2 cells, and with 680C91 or CH-223191 after 36 h (left, representative pictures; right, bar charts indicating the cell numbers of migration cells. Magnification 100 ×). (F) Representative images of foci formation in monolayer cultures of vector, TDO2 cells, and with 680C91 or CH-223191, and the number of colonies detected. 500 cells per well were seeded onto 6-well plates, and images of foci formation were taken after 10 days of culture. The results are expressed as the mean ± SEM, $n = 3$; $^{**}P < 0.01$ and $^{***}P < 0.001$.

could promote tumor progression. KYSE150 and KYSE450 were treated with increasing doses of KYN for over 3 days. Indeed, we found that dose-dependent effect of exogenous KYN application promoted tumor cells proliferate (Supporting Information Fig. S3). Therefore, we determined 30 and 60 μmol/L KYN to test whether KYN acts tumor cells to affect tumor progression. As shown in Fig. 3, at the concentration of 30 and 60 μmol/L, KYN could promote the proliferation and migration, but not colony formation of KYSE150 and KYSE450 cells, demonstrating the direct impact of KYN on ESCC cells.

3.3. *TDO2-AHR axis promotes ESCC tumorigenesis*

To further validate the effect of TDO2 on tumor growth *in vivo*, tumor xenografts in nude mice were established by subcutaneous injection of KYSE150-TDO2 cells and KYSE150-Vector control cells into the right dorsal flank of mice. It was found that the tumor volumes in KYSE150-TDO2 group were significantly larger than that in the control group. As showed in Fig. 4A, treatment of mice with 680C91 (5 mg/kg, pH = 2.5) or CH-223191 (10 mg/kg in corn oil) significantly prevented the tumor growth of KYSE150-TDO2 group. Even though the expression of TDO2 was low in KYSE150-Vector cells, TDO2 expression could be detected in KYSE150-Vector tumor xenograft *in vivo* (Supporting Information Fig. S4C). The reduction in tumor volume in response to treatment with CH-223191 confirmed the aberrant stimulation of AHR by KYN produced through TDO2 in ESCC cells (Fig. 4A). These results implicate that TDO2 could promote the tumor growth *in vivo*. To further investigate whether TRP catabolism was altered, the concentrations of serum KYN of tumor bearing mice were detected by using HPLC. The concentration of KYN in KYSE150-TDO2 group (106.32 ± 48.69 μmol/L) was higher than that in the control group (69.73 ± 7.73 μmol/L). Meanwhile, the concentration of serum KYN in mice receiving 680C91 was 43.02 ± 14.65 μmol/L and 48.36 ± 25.44 μmol/L in mice receiving CH-223191 (Fig. 4B). We also assessed the serum TRP levels in this study (Fig. S4A). Therefore, TDO2 in ESCC could significantly increase KYN, whereas the effect was significantly abrogated by TDO2 inhibitor

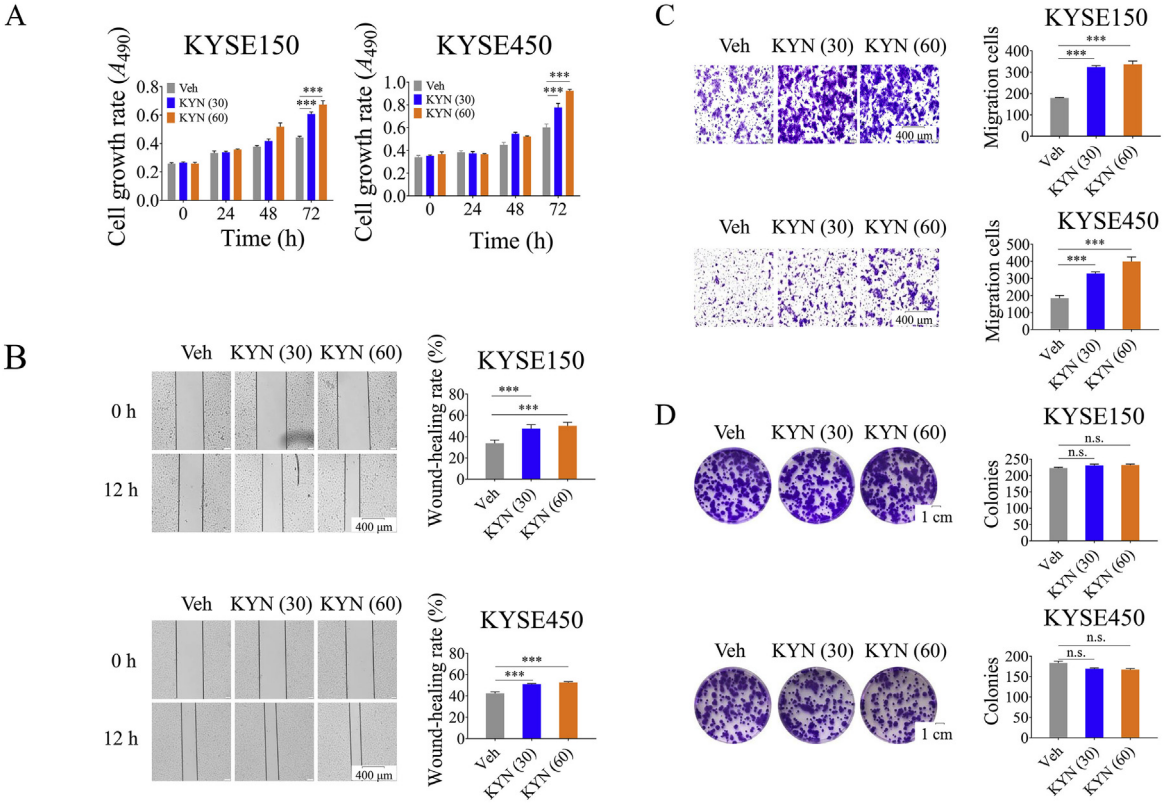

Figure 3 Effects of KYN on proliferation and migration of ESCC cells. (A) Cell growth rates of KYSE150 and KYSE450 treated with Veh (0.1% DMSO), 30 and 60 μmol/L KYN, respectively. (B) Wound-healing assay. Representative wound closing cells (12 h) after scratching (0 h) of KYSE150 and KYSE450 treated with Veh (0.1% DMSO), 30 and 60 μmol/L KYN, respectively. (left, representative pictures; right, bar charts indicating the wound-healing rate. Magnification 100 ×). (C) Transwell assays for migration of KYSE150 and KYSE450 treated with Veh (0.1% DMSO), 30 and 60 μmol/L KYN, respectively. (left, representative pictures; right, bar charts indicating the cell numbers of migration cells. Magnification 100 ×). (D) Representative images of foci formation in monolayer cultures of KYSE150 and KYSE450 treated with Veh (0.1% DMSO), 30 and 60 μmol/L KYN, respectively, and the number of colonies detected. Experiments were conducted as we described above. The results are expressed as the mean ± SEM, $n = 3$; n.s., not significant; ***$P < 0.001$.

680C91 or AHR antagonist CH-223191, indicating there might be a positive feedback.

To investigate whether TDO2 promotes the progression of primary tumor of ESCC, a putative primary ESCC model induced by 4-NQO was established as shown in Fig. 5A. As the tumor progression induced by 4-NQO, the body weight of tumor bearing mice significantly decreased, while treatment with 680C91 ($P < 0.05$) or CH-223191 ($P < 0.05$) could maintain the body weight of mice compared with the untreated group (Fig. 5B). Consistently, the average tumor numbers of the untreated group (5.6 ± 0.8) were significantly higher than those of 680C91 group (2 ± 0.63) and CH-223191 group (1.4 ± 0.8) (Fig. 5C). In addition, lower KYN concentrations were detected in the serum of ESCC mice treated with 680C91 or CH-223191, as shown in Fig. 5D. Serum TRP levels in ESCC mice were detected by using HPLC (Fig. S4B). These results suggest that inhibition of TDO2−AHR pathway could reduce the tumorigenesis of ESCC in both xenograft model and 4-NQO induced primary model.

3.4. *TDO2 promotes ESCC M2 macrophages polarization*

Multiple mechanisms of immune suppression can arise in the tumor to facilitate the progression of cancer[39]. Among them, tumor polarization of M2 macrophages represents one major impediment to effective antitumor immune responses. According to the previous report, KYN produced by glioblastoma cells activates AHR to modulate M2 macrophages activation[40]. Therefore, we also analyzed the changes of macrophages in the progress of tumor growth promoted by TDO2 in a xenograft nude mice model. The results indicate that the percentage of M1 macrophages showed no difference (Fig. 4C). In contrast, the percentage of M2 macrophages was higher in xenograft tumors with stably overexpression of TDO2, which was significantly inhibited by the treatment of 680C91 or CH-223191 (Fig. 4D). To verify the role of tumor-associated macrophages (TAM) in the tumor progression by TDO2, a macrophage depletion model was established with the liposome CCL, and CNL as control.

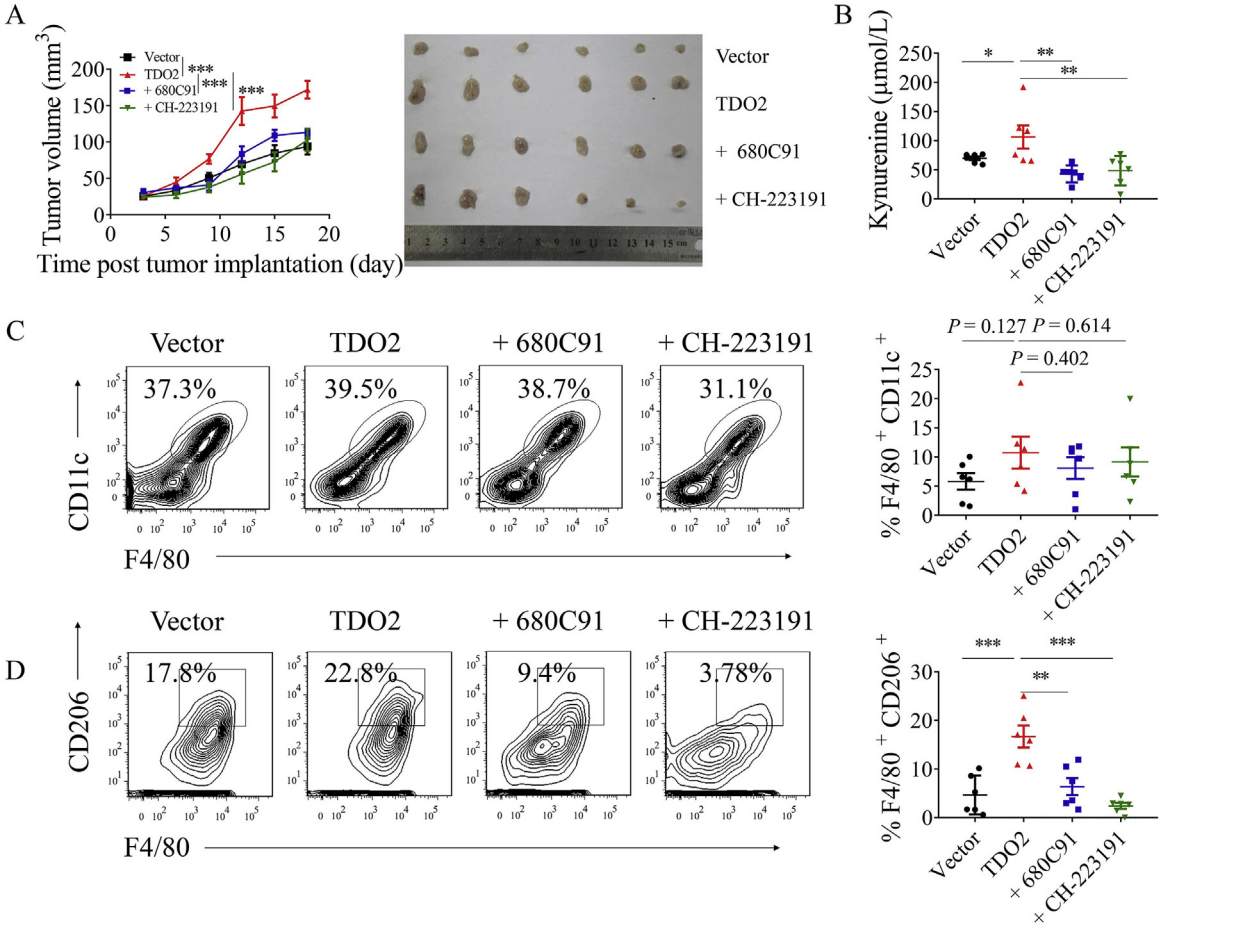

Figure 4 TDO2 expression degrades to KYN and increases its effects on tumorigenicity, induces M2 infiltration in nude mice. (A) Volume of xenograft tumors of the nude mice incubated with either Vector or TDO2 cells were detected at 3, 6, 9, 12, 15, and 18 days. 680C91 was given at 15 mg/kg orally every three days, and CH-223191 was given at 10 mg/kg by oral gavage every three days, beginning at the first day of tumor implantation. (B) Higher serum levels of KYN were detected in mice bearing KYSE150-TDO2 compared with KYSE150-Vec, and 680C91 or CH-223191 treatment. Infiltration of M1 macrophages (C) and M2 macrophages (D) in $CD45^+$ cells were analyzed after administration of 680C91 or CH-223191 using flow cytometry. All data are displayed as mean ± SEM, $n = 6$; $P > 0.05$, not significant; $^*P < 0.05$; $^{**}P < 0.01$ and $^{***}P < 0.001$.

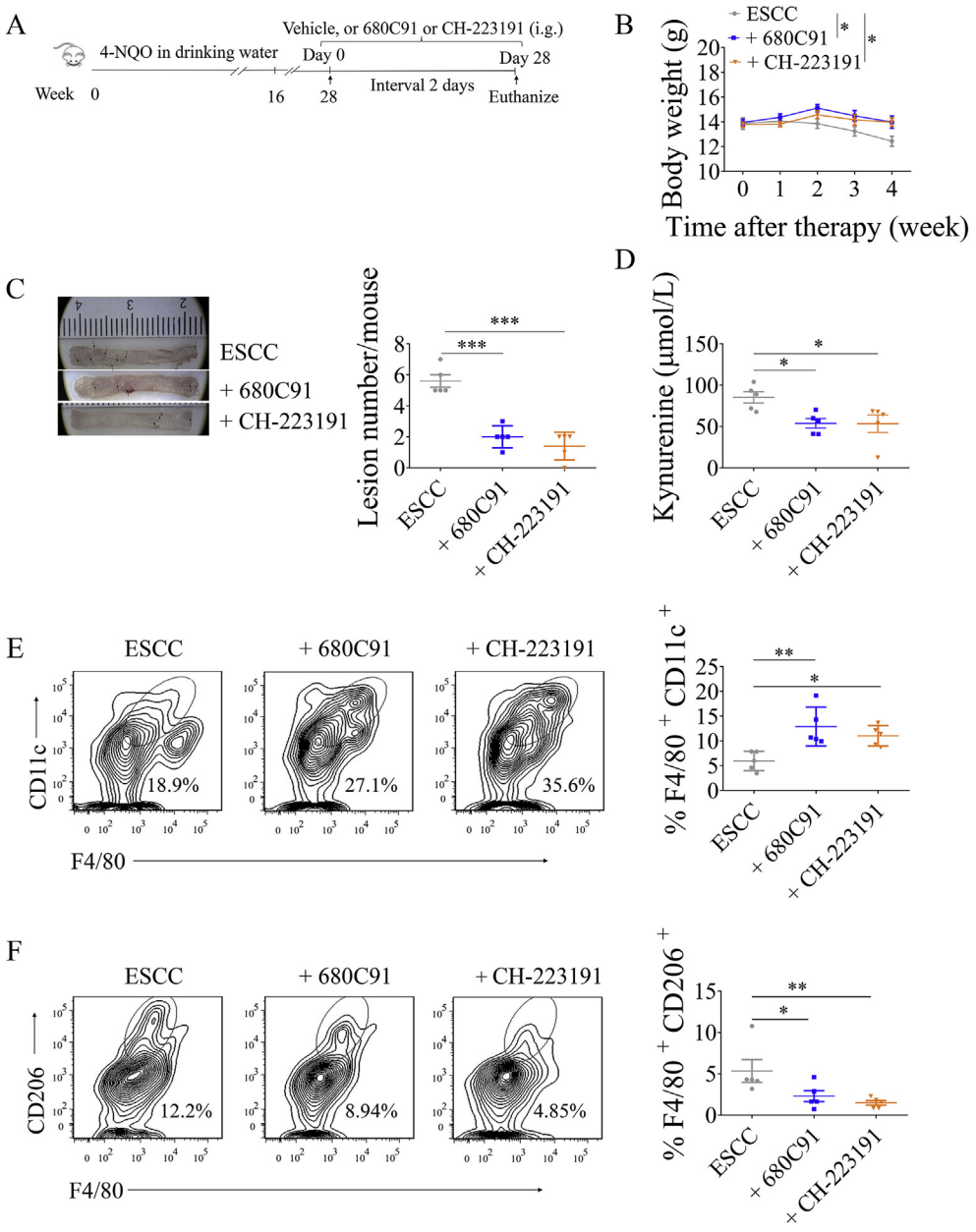

Figure 5 TDO2 affects tumor burden and induces monocyte differentiation into M2 macrophages *via* AHR in ESCC model tumors. (A) Experimental regimen for the ESCC model used in (B)−(F). (B) Body weight changes with or without 680C91 and CH-223191 from Week 29 to Week 32 measured every three days. (C) Representative esophagi with polys (left panel) and tumor quantification (right panel). (D) KYN secretion levels in mice serum, as measured by HPLC, from 4-NQO induced ESCC mice and 680C91 or CH-223191 treatment. Changes of M1 macrophages (E) and M2 macrophages (F) of $CD45^+$ cells of esophageal in ESCC mice exposed to 4-NQO, treated by 680C91 or CH-223191. All data are displayed as mean ± SEM, $n = 5$; $^*P < 0.05$; $^{**}P < 0.01$ and $^{***}P < 0.001$.

The data of the efficiency of macrophage-depletion by CCL were shown in Fig. S4D and S4E. Consist with the results above, TDO2 significantly promoted the tumor progression compared with the vector group. Further, with the macrophage depletion, the tumor progression by TDO2 overexpression was abolished (Fig. 6F). Interestingly, the depletion of macrophages completely blocked the pro-tumor activity of TDO2 (Fig. 6F), which led us to hypothesize that B cells, NK cells and granulocytes existing in nude mice might resist tumor cells with macrophages depleted. It was found that the tumor volumes treated with CCL were significantly smaller than that in the CNL group. Thus, these results confirm our observations *in vivo*, leading further support to our hypothesis that macrophages were required for tumor growth induced by TDO2.

In the 4-NQO induced ESCC model, we found that there was a moderate increase of M1 macrophages in 680C91 and CH-223191 treatment group (Fig. 5E). Meanwhile, treatment with 680C91 and CH-223191 significantly inhibited the percentages of M2 macrophage (Fig. 5F). We next found that TDO2 gene expression was also associated with M2 macrophage markers by analyzing publicly available datasets from TCGA (Supporting Information Fig. S5). Thus, both in the presence and absence of adaptive

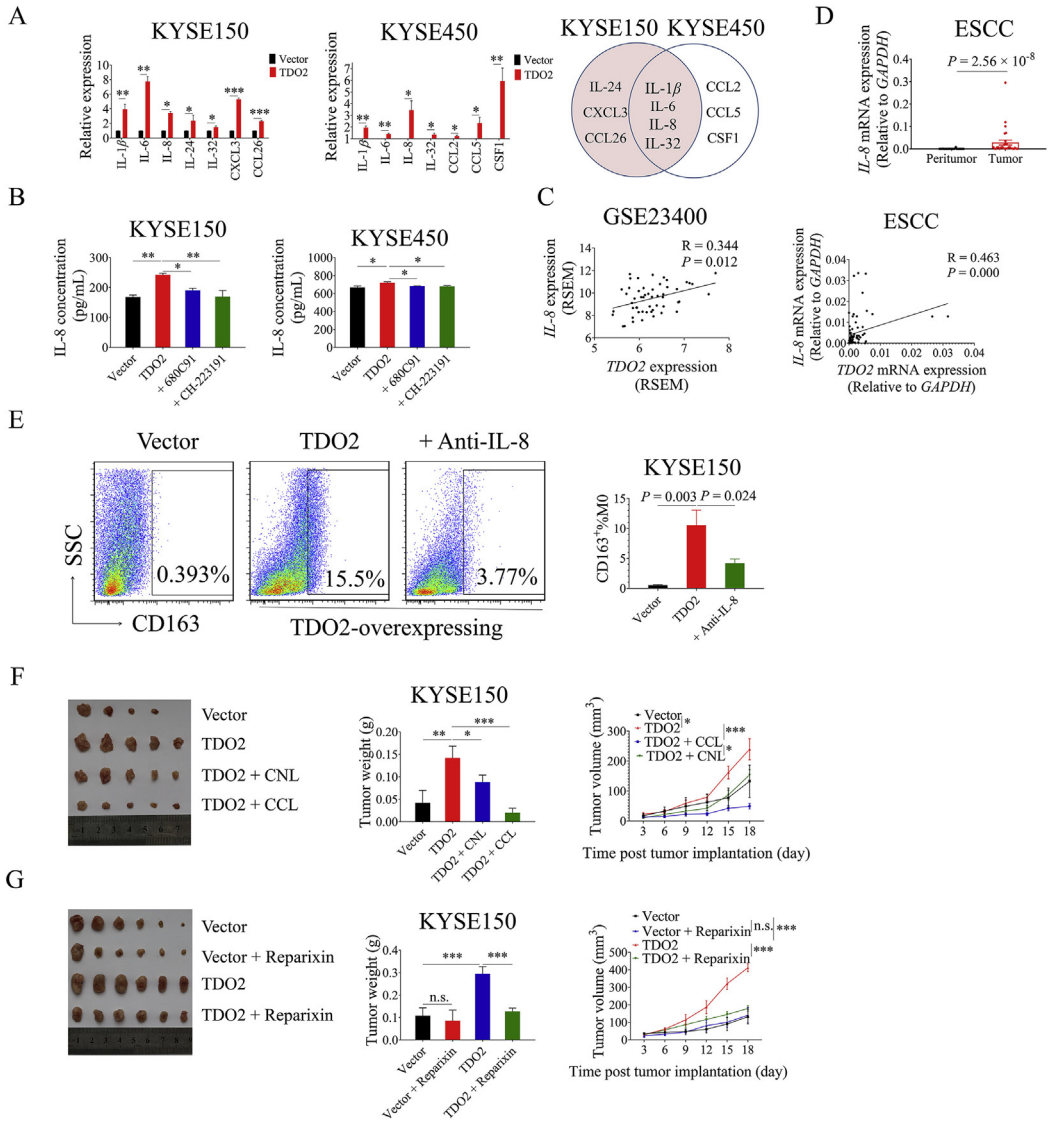

Figure 6 TDO2-induced IL-8 activated M2 polarization of TAM promoting a phenotype switch. (A) Detection of cytokines and chemokines by qRT-PCR in TDO2-overexpressed and vector-transfected KYSE150 (left panel) and KYSE450 (right panel). Gene expression is represented as relative values normalized to *GAPDH*. Venn diagram (lower panel) of chemokines and cytokines that changed significantly (detected by qRT-PCR) both in KYSE150 and KYSE450 cells. (B) The concentration of IL-8 in the culture medium was detected by ELISA between TDO2-overexpressed and control cells cultured for 36 h when cells were treated TDO2 inhibitor (680C91) and AHR inhibitor (CH-223191). (C) Gene expression correlation between *TDO2* and *IL-8* in GEO dataset (GSE23400, left panel) and human ESCC (right panel) by qRT-PCR analysis. Each spot represents one ESCC patient. (D) Relative mRNA levels of *IL-8* were examined by qRT-PCR analysis in 30 pairs of ESCC and paired normal samples. (E) PBMCs were co-cultured with KYSE150-vector, KYSE150-TDO2 cells and treated with or without anti-IL-8 neutralized antibody. (F) Volumes and weights of xenograft tumors from nude mice injected with vector, TDO2-overexpressing cells were detected at 3, 6, 9, 12, 15, and 18 days. (G) Effects of reparixin on tumor volume and tumor weight in KYSE150 xenograft mouse model. Reparixin (30 mg/kg) or control (saline) were injected subcutaneously every 3 days for 18 days. The middle and right panels show tumor weight and volume in vector, vector+reparixin, TDO2, TDO2+reparixin groups. All data are displayed as mean ± SEM, $n = 5$ or 6; $^{*}P < 0.05$; $^{**}P < 0.01$ and $^{***}P < 0.001$.

immunity, TDO2 activity could promote the polarization or recruitment of M2 macrophages by producing KYN to function through AHR.

3.5. *Overexpression of TDO2 promotes IL-8 secretion*

Cytokines and chemokines play a vital role during the progression of cancers. Accumulating evidence suggested that TDO2 could promote the expression of AHR-regulated genes including cytokines and chemokines[12]. To elucidate whether these factors were involved to increase the M2 macrophages in ESCC, we detected 13 cytokines, 17 chemokines and 3 inflammatory cytokines using qRT-PCR and found that the expression of IL-1β, IL-6, IL-8 and IL-32 were significantly increased in TDO2-overepressed cells (Fig. 6A and Supporting Information Fig. S6A). Only IL-8 was upregulated in TDO2-

overexpressed cells confirmed by ELISA, while either inhibition of TDO2 or AHR could reduce the production of IL-8, whereas IL-6 was not (Fig. 6B and Fig. S6B). In addition, IL-32 secretion was not detected in TDO2-overexpressed cells (data were not shown). All these results indicate that IL-8 might be a downstream target of TDO2 in ESCC.

Moreover, the expression of IL-8 in ESCC was identified to be positively correlated with TDO2 at the mRNA level by analyzing GEO dataset, which was also verified by using fresh tissues of ESCC (Fig. 6C). IL-8 was reported to promote an anti-inflammatory microenvironment by inducing M2 macrophages[21,34,41]. Additionally, we found that the expression of IL-8 was significantly higher than that of the adjacent normal tissues in our samples and GEO database (Fig. 6D and Fig. S6C). As shown in Fig. 6E, addition of anti-IL8 (20 μg/mL) to the conditioned medium of KYSE150-TDO2 cells could partly abrogate the enhancement effect of TDO2 on macrophage polarization. Next, we systematically assessed whether IL-8 was required to TDO2-derived tumor progression. To do so, in nude mice-bearing KYSE-puro and KYSE150-TDO2 tumor xenografts, mice received a subcutaneous injection of reparixin (IL-8R inhibitor, 30 mg/kg). As shown in Fig. 6G, reparixin significantly decreased the tumor growth of KYSE150-TDO2 group and we found inhibitor of IL-8 had no effect on KYSE150-puro group. In conclusion, TDO2 might promote ESCC progression through IL-8-regulated M2 macrophage polarization.

3.6. KYN could induce IL-8 production by activating the AKT/GSK3β pathway

Kumar et al.[42] demonstrates that KYN can activate the AKT/GSK3β signaling pathway in neoplastic colon epithelium, which has been reported to regulate IL-8 secretion[43]. To investigate whether KYN can activate this pathway in ESCC, we firstly divided the 98 ESCC samples in TCGA into low expression group and high expression group according to the expression level of TDO2, and the transcriptome data between these two groups was compared. The key cellular processes and signal pathways of TDO2 in ESCC were identified by gene set enrichment analysis (GSEA). GSEA showed that the enriched genes were related to chemokine activity, cytokine secretion, inflammatory response, IL-6/JAK/STAT3 signal pathway, Biocarta GSK3β signal pathway, and EGFR signal pathway (Supporting Information Fig. S7A and S7B). We thus wondered whether KYN/AHR would trigger AKT/GSK3β signaling pathway in the ESCC cell lines. As shown in Fig. 7A, the mean concentration of IL-8, as determined by ELISA, was elevated significantly in response to treatment with 60 μmol/L KYN or overexpression TDO2 compared with control cells, demonstrating that TDO2-mediated KYN production could induce IL-8 production. KYSE150 and KYSE450 were treated with 60 μmol/L KYN, and the expression of p-AKT and p-GSK3β were observed by western blot (Fig. 7B). To further demonstrate that TDO2 mediates AKT/GSK3β activation was through AHR, tumor cells were treated with inhibitor of AHR, AKT, GSK3β. In-line with previous reports, we revealed that CH-223191 could downregulate phosphorylated AKT, phosphorylated GSK3β and IL-8 production (Fig. 7A−C). An AKT inhibitor (AZD5363, AZD) could also downregulate phosphorylated GSK3β and IL-8 production, with p-AKT phosphorylated but catalytically inactive (Fig. 7A and C)[44]. The GSK3β inhibitor (CHIR-99021, CHIR) could downregulated phosphorylated GSK3β and secretion of IL-8 (Fig. 7A and C). Therefore, we could infer that the oncogenic function of TDO2 is to upregulate IL-8 production for the polarization of M2 macrophages *via* activation of the AKT/GSK3β pathway.

AZD5363 and CHIR-99021, the small molecules which selectively inhibited activation of AKT and GSK3β, were used to inhibit the phosphorylated of AKT and GSK3β. The results showed that AZD5363 and CHIR-99021 effectively diminished proliferation, migration and colony formation, which were increased by TDO2 (**$P < 0.01$ and ***$P < 0.001$; Fig. 7D−G). Therefore, it could be inferred that the oncogenic function of TDO2/KYN/AHR axis in ESCC was to upregulate IL-8 for polarization of M2 macrophages *via* activation of AKT/GSK3β signaling pathway.

4. Discussion

Esophageal squamous cell carcinoma ranks as the fourth leading cause of cancer-related death and the eighth most commonly diagnosed malignant cases in China[45,46]. Despite the advances in multimodality therapy, the prognosis of ESCC has been very dismal in the past several decades due to a high probability of invasion and metastasis. Thus, it is urgent to identify new therapeutic targets through understanding the molecular mechanism for ESCC.

Accumulating evidence has demonstrated that TME plays a crucial role in the development and progression of many cancers. IDO1 and TDO2 catalyze the commitment step of kynurenine metabolic pathway and foster an immune-suppressing tumor microenvironment which is defective in recognizing and eradicating cancer cells. Although TDO2 expression was detected at relative low level in ESCC cell lines, the expression of TDO2 could be detected both in tumor cells of ESCC tumors and KYSE150-vector tumor xenograft *in vivo*. We can infer that the expression of TDO2 in tumor tissues different from tumor cell lines might be due to the discrepancy between *in vitro* and *in vivo*. The present study revealed that TDO2 is overexpressed in ESCC tissues, which is much more significant than that of IDO1. There are strong correlations between the high level of TDO2 and gender, TNM stage, lymph node metastasis, and poor survival of patients with ESCC[37]. TRP was reported to be ultimately metabolized to KYN, QA, and PA by TDO2 and contribute to neoplastic pathogenesis in some models[12,42]. But our results demonstrate that KYN is the most highly increased metabolite in conditioned media from TDO2-overexpressed ESCC cells, thus we hypothesized that ESCC cells might utilize an autocrine signaling loop in which KYN activated AHR to support their proliferation and migration. Inhibition of TDO2 or AHR decreased the proliferation, migration and colony formation of KYSE150-TDO2 and KYSE450-TDO2 cells. Furthermore, the tumorigenic ability of KYSE150 was promoted by TDO2, while inhibitors of TDO2 or AHR decreased tumor volumes and esophageal tumorigenesis. All these revealed that TDO2 might promote carcinogenesis and progression in ESCC and be a potential therapeutic target for ESCC.

We further discovered that TDO2-AHR to be a key mediator of M2 macrophages recruitment in ESCC. In addition to its autocrine role described above, KYN could facilitate tumor progression through paracrine signaling mechanisms involving suppression of immune surveillance. Specifically, the AHR signaling that is triggered by glioma-secreted KYN controls M2 macrophages

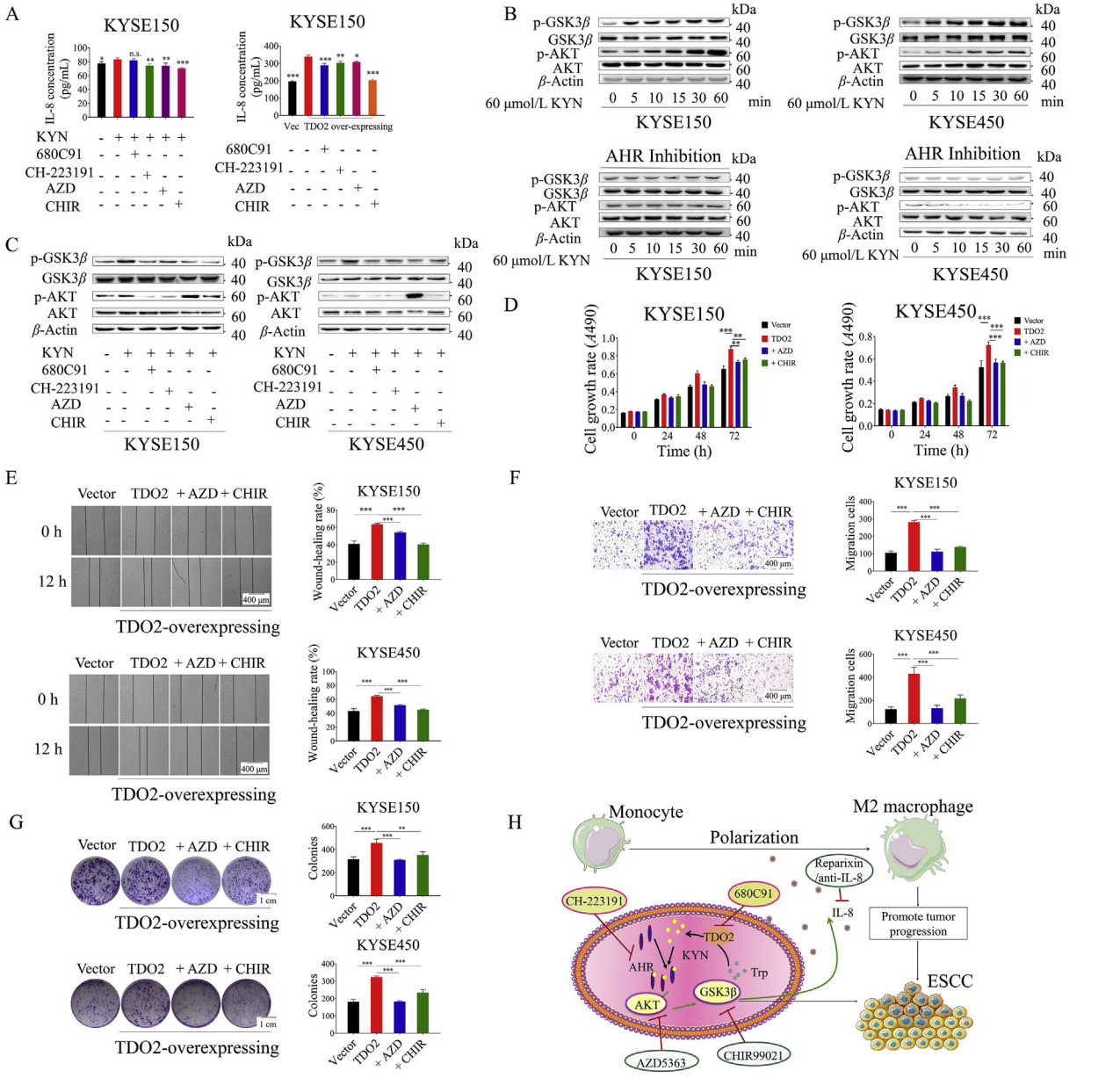

Figure 7 KYN rapidly actives AKT/GSK3β signaling pathway *via* AHR. (A) The secretion of IL-8 was detected by ELISA when cells were treated with KYN, TDO2 inhibitor (680C91), AHR inhibitor (CH-223191), AKT inhibitor (AZD) and GSK3β inhibitor (CHIR). (B) KYSE150 and KYSE450 ESCC cells were treated with KYN for specified time points, followed by whole-cell protein extraction (upper panel). Western blot was performed to analyze the phosphorylation levels of AKT-Ser473 and GSK3β-Ser9. Inhibition of AHR with CH-223191 prevented AKT and GSK3β activation in with KYSE150 and KYSE450 cells (lower panel). (C) The expression of AKT, p-AKT, GSK3β and p-GSK3β by Western blot when cells were treated with KYN, TDO2 inhibitor (680C91), AHR inhibitor (CH-223191), AKT inhibitor (AZD) and GSK3β inhibitor (CHIR). Treated with AZD or CHIR decreased cell growth rates (D), migration (E) and (F) and colony formation (G) of tumor cells. The results are expressed as the mean ± SEM, $n = 3$; n.s., not significant; *$P < 0.05$, **$P < 0.01$ and ***$P < 0.001$. (H) Schematic depicting dual functions of TDO2 in ESCC.

polarization by partially driving CCR2 expression[40]. Our observation in ESCC in nude mice lack of mature T cells suggested that TDO2 could promote the polarization of M2 macrophages and tumor growth independent of its impact on adaptive immunity. Tumor volumes of the nude mice treatment with CCL were significantly smaller than those of CNL group, demonstrating that macrophages play a vital role in abrogating pro-tumor activity of TDO2. However, in light of our observation in M1 macrophages, it is intriguing to reason that TDO2 does not regulate in M1 macrophages infiltration in mice lacking intact adaptive immunity. Collectively, our results suggest that in ESCC, TDO2 is an important contributor to KYN production, and thus activates AHR to promote M2 macrophages polarization and disease progression[40,47–50].

Multiple cytokines and chemokines relevant to AHR activation are thought to be correlated with tumor progression[12,51]. In the GBM model, AHR could affect the recruitment of M2 macrophages

via CCL2 and CCR2 and other mediator molecules[40]. We hypothesized that the overexpression of TDO2 in ESCC utilizes a signaling loop in which KYN activates AHR to secret cytokines or chemokines in modulating the polarization of M2 macrophages. Previous studies on TDO2 have focused on its impact on immune-tolerant dendritic cells and regulatory T cells[52,53], with little attention paid to its possible role in the TAM of ESCC. As a part of the concerted mechanisms of evading immune surveillance, numerous types of cancers cells upregulate TDO2 and induce immune tolerant effect *via* TRP starvation and activates AHR to promote the transcription of IL-1A, IL-1B, IL-6, and IL-10[12,52]. In order to investigate whether TDO2 also functions through the chemokines or cytokines in TME of ESCC, we found that only IL-8 was significantly changed in TDO2 overexpressed ESCC cell lines or tumor cells treated with KYN. Intriguing studies implicated that autocrine IL-8 produced by tumor cells could recruit monocytes and stimulate their differentiation into tumor-promoting M2-like macrophages[54−56]. Importantly, our results shed light on observational studies linking TDO2 expression in ESCC with IL-8 from in-house and public available datasets. Our observation revealed that inhibition of TDO2 or AHR decreased the ability of KYSE150-TDO2 and KYSE450-TDO2 cells to secret IL-8 *in vitro*. In our experiments, we found blocking IL-8 and depletion of macrophage abrogated pro-tumor activity of TDO2. Collectively, these results indicated that TDO2-mediated KYN production could up-regulated IL-8, which promoted the polarization of M2 macrophages to support immune escape of cancer cells.

Nonetheless, the molecular mechanism of TDO2-regulated IL-8 has not been elucidated. In colorectal cancer, IDO1-KYN metabolites can promote nuclear translocation of β-catenin, cellular proliferation, and resistance to apoptosis *via* activation of AKT/GSK3β signaling[42]. Furthermore, MAEL could upregulate IL-8 to promote tumor progression *via* activation of AKT signaling pathway[43]. Therefore, we hypothesized that TDO2 could regulate IL-8 *via* AKT/GSK3β in ESCC as well. Our data demonstrate that expression of AKT-dependent GSK3β phosphorylation and IL-8 production rapidly increased when AHR was activated, while opposite results were observed when AHR was inhibited. The secretion of IL-8, active or phosphorylated AKT and phosphorylated GSK3β were decreased when cells were treated with AZD5363 and CHIR-99021. Moreover, the proliferation, migration and colony formation of TDO2-overexpression cells markedly decreased after treated with AZD5363 or CHIR-99021. Therefore, the influence of AHR activation by KYN or over-expression TDO2 on IL-8 and further the polarization of M2 macrophages could be mediated through regulating AKT/GSK3β signaling, and provides a new paradigm in TDO2-mediated cancer progression.

The role of TDO2 in 4-NQO induced ESCC model has not been previously described. To investigate the role of TDO2 in chronic 4-NQO-associated tumorigenesis, we used usual doses of 680C91 and CH-223191. TDO2 inhibition with 680C91 or AHR inhibition with CH-223191 did reduce tumor burden. Still, these findings are intriguing and potentially suggest that shunting of the AHR pathway may have a potential to inhibit ESCC tumorigenesis.

5. Conclusions

In summary, our results demonstrate that TDO2 expression plays a vital role in the development and progression of ESCC. These findings provide mechanistic evidence to support the association of high expression level of TDO2 and poor prognosis of human ESCC in the retrospective studies. Our results provide new insight into the adaptive survival advantage of TDO2 by showing that TDO2 directly promotes tumor growth and proliferation of the neoplastic epithelium both in the presence and absence of adaptive immunity. Studies both *in vivo* and *in vitro* showed that TDO2 promoted proliferation, migration, colony formation and promoted M2 macrophages polarization by activating the AKT/GSK3β/IL-8 signaling pathway. These findings provide evidence that TDO2 is an important molecule participating in the aberrant activation of AKT/GSK3β signaling pathway and thus may serve as a potential therapeutic target for treating ESCC.

Acknowledgments

This work was supported by the National Natural Science Foundation of China (Nos. U1604286, 81822043, and 81901687), Shenzhen Science and Technology Program (3000531, China), and the Key Incubation Fund of SYSU (19ykzd29, China).

Author contributions

Yuanming Qi and Yanfeng Gao conceived and designed the experiments. Yumiao Zhao performed the experiments. Jiaxin Sun, Yin Li, Xiuman Zhou, Wenjie Zhai, Yahong Wu, Guanyu Chen, Shanshan Gou, Xinghua Sui, Wenshan Zhao, Lu Qiu, Yongjie Yao, Yixuan Sun and Chunxia Chen helped to perform the experiments. Yumiao Zhao, Jiaxin Sun, Yuanming Qi and Yanfeng Gao analyzed and interpreted the results. All authors wrote the manuscript with inputs from all authors, discussed the results and gave final approval of the manuscript.

Conflicts of interest

The authors declare no conflicts of interest.

Appendix A. Supporting information

Supporting data to this article can be found online at https://doi.org/10.1016/j.apsb.2021.03.009.

References

1. Global Burden of Disease Cancer C, Fitzmaurice C, Akinyemiju TF, Al Lami FH, Alam T, Alizadeh-Navaei R, et al. Global, regional, and national cancer incidence, mortality, years of life lost, years lived with disability, and disability-adjusted life-years for 29 cancer groups, 1990 to 2016: a systematic analysis for the global burden of disease study. *JAMA Oncol* 2018;**4**:1553−68.
2. Arnold M, Soerjomataram I, Ferlay J, Forman D. Global incidence of oesophageal cancer by histological subtype in 2012. *Gut* 2015;**64**:381−7.
3. Ma WW, Xie H, Fetterly G, Pitzonka L, Whitworth A, LeVea C, et al. A phase Ib study of the FGFR/VEGFR inhibitor dovitinib with gemcitabine and capecitabine in advanced solid tumor and pancreatic cancer patients. *Am J Clin Oncol* 2019;**42**:184−9.
4. Paz-Ares L, Tan EH, O'Byrne K, Zhang L, Hirsh V, Boyer M, et al. Afatinib *versus* gefitinib in patients with EGFR mutation-positive advanced non-small-cell lung cancer: overall survival data from the phase IIb LUX-Lung 7 trial. *Ann Oncol* 2017;**28**:270−7.
5. Kang X, Chen K, Li Y, Li J, D'Amico TA, Chen X. Personalized targeted therapy for esophageal squamous cell carcinoma. *World J Gastroenterol* 2015;**21**:7648−58.

6. Guagnano V, Kauffmann A, Wohrle S, Stamm C, Ito M, Barys L, et al. FGFR genetic alterations predict for sensitivity to NVP-BGJ398, a selective pan-FGFR inhibitor. *Cancer Discov* 2012;**2**:1118−33.
7. Santhanam S, Alvarado DM, Ciorba MA. Therapeutic targeting of inflammation and tryptophan metabolism in colon and gastrointestinal cancer. *Transl Res* 2016;**167**:67−79.
8. Greene LI, Bruno TC, Christenson JL, D'Alessandro A, Culp-Hill R, Torkko K, et al. A role for tryptophan-2,3-dioxygenase in CD8 T-cell suppression and evidence of tryptophan catabolism in breast cancer patient plasma. *Mol Cancer Res* 2019;**17**:131−9.
9. El-Zaatari M, Bass AJ, Bowlby R, Zhang M, Syu LJ, Yang Y, et al. Indoleamine 2,3-dioxygenase 1, increased in human gastric preneoplasia, promotes inflammation and metaplasia in mice and is associated with type II hypersensitivity/autoimmunity. *Gastroenterology* 2018;**154**:140−153.e17.
10. Zhu Y, Li M, Bo C, Liu X, Zhang J, Li Z, et al. Prognostic significance of the lymphocyte-to-monocyte ratio and the tumor-infiltrating lymphocyte to tumor-associated macrophage ratio in patients with stage T3N0M0 esophageal squamous cell carcinoma. *Cancer Immunol Immunother* 2017;**66**:343−54.
11. D'Amato NC, Rogers TJ, Gordon MA, Greene LI, Cochrane DR, Spoelstra NS, et al. A TDO2-AhR signaling axis facilitates anoikis resistance and metastasis in triple-negative breast cancer. *Cancer Res* 2015;**75**:4651−64.
12. Opitz CA, Litzenburger UM, Sahm F, Ott M, Tritschler I, Trump S, et al. An endogenous tumour-promoting ligand of the human aryl hydrocarbon receptor. *Nature* 2011;**478**:197−203.
13. Belladonna ML, Grohmann U, Guidetti P, Volpi C, Bianchi R, Fioretti MC, et al. Kynurenine pathway enzymes in dendritic cells initiate tolerogenesis in the absence of functional IDO. *J Immunol* 2006;**177**:130−7.
14. Gonzalez FJ, Fernandez-Salguero P, Ward JM. The role of the aryl hydrocarbon receptor in animal development, physiological homeostasis and toxicity of TCDD. *J Toxicol Sci* 1996;**21**:273−7.
15. Stone TW, Darlington LG. Endogenous kynurenines as targets for drug discovery and development. *Nat Rev Drug Discov* 2002;**1**:609−20.
16. Kiyozumi Y, Baba Y, Okadome K, Yagi T, Ishimoto T, Iwatsuki M, et al. IDO1 expression is associated with immune tolerance and poor prognosis in patients with surgically resected esophageal cancer. *Ann Surg* 2019;**269**:1101−8.
17. Liu J, Lu G, Tang F, Liu Y, Cui G. Localization of indoleamine 2,3-dioxygenase in human esophageal squamous cell carcinomas. *Virchows Arch* 2009;**455**:441−8.
18. Rosenberg AJ, Wainwright DA, Rademaker A, Galvez C, Genet M, Zhai L, et al. Indoleamine 2,3-dioxygenase 1 and overall survival of patients diagnosed with esophageal cancer. *Oncotarget* 2018;**9**:23482−93.
19. Kristeleit R, Davidenko I, Shirinkin V, El-Khouly F, Bondarenko I, Goodheart MJ, et al. A randomised, open-label, phase 2 study of the IDO1 inhibitor epacadostat (INCB024360) *versus* tamoxifen as therapy for biochemically recurrent (CA-125 relapse)-only epithelial ovarian cancer, primary peritoneal carcinoma, or fallopian tube cancer. *Gynecol Oncol* 2017;**146**:484−90.
20. Triplett TA, Garrison KC, Marshall N, Donkor M, Blazeck J, Lamb C, et al. Reversal of indoleamine 2,3-dioxygenase-mediated cancer immune suppression by systemic kynurenine depletion with a therapeutic enzyme. *Nat Biotechnol* 2018;**36**:758−64.
21. Xu Y, Liao C, Liu R, Liu J, Chen Z, Zhao H, et al. IRGM promotes glioma M2 macrophage polarization through p62/TRAF6/NF-κB pathway mediated IL-8 production. *Cell Biol Int* 2019;**43**:125−35.
22. Xu Y, Cui G, Jiang Z, Li N, Zhang X. Survival analysis with regard to PD-L1 and CD155 expression in human small cell lung cancer and a comparison with associated receptors. *Oncol Lett* 2019;**17**:2960−8.
23. Cassetta L, Pollard JW. Targeting macrophages: therapeutic approaches in cancer. *Nat Rev Drug Discov* 2018;**17**:887−904.
24. Lee CL, Guo Y, So KH, Vijayan M, Guo Y, Wong VH, et al. Soluble human leukocyte antigen G5 polarizes differentiation of macrophages toward a decidual macrophage-like phenotype. *Hum Reprod* 2015;**30**:2263−74.
25. Li X, Song Y, Liu F, Liu D, Miao H, Ren J, et al. Long non-coding RNA MALAT1 promotes proliferation, angiogenesis, and immunosuppressive properties of mesenchymal stem cells by inducing VEGF and IDO. *J Cell Biochem* 2017;**118**:2780−91.
26. Abreu SC, Xisto DG, de Oliveira TB, Blanco NG, de Castro LL, Kitoko JZ, et al. Serum from asthmatic mice potentiates the therapeutic effects of mesenchymal stromal cells in experimental allergic asthma. *Stem Cells Transl Med* 2019;**8**:301−12.
27. Qiu L, Wang M, Hu S, Ru X, Ren Y, Zhang Z, et al. Oncogenic activation of Nrf2, though as a master antioxidant transcription factor, liberated by specific knockout of the full-length nrf1alpha that acts as a dominant tumor repressor. *Cancers (Basel)* 2018;**10**:520.
28. Zhou XM, Li WQ, Wu YH, Han L, Cao XG, Yang XM, et al. Intrinsic expression of immune checkpoint molecule TIGIT could help tumor growth *in vivo* by suppressing the function of NK and $CD8^+$ T Cells. *Front Immunol* 2018;**9**:2821.
29. Liu Y, Liu L, Zhou Y, Zhou P, Yan Q, Chen X, et al. CKLF1 enhances inflammation-mediated carcinogenesis and prevents doxorubicin-induced apoptosis *via* IL6/STAT3 signaling in HCC. *Clin Cancer Res* 2019;**25**:4141−54.
30. Sousa S, Brion R, Lintunen M, Kronqvist P, Sandholm J, Monkkonen J, et al. Human breast cancer cells educate macrophages toward the M2 activation status. *Breast Cancer Res* 2015;**17**:101.
31. Pilotte L, Larrieu P, Stroobant V, Colau D, Dolusic E, Frederick R, et al. Reversal of tumoral immune resistance by inhibition of tryptophan 2,3-dioxygenase. *Proc Natl Acad Sci U S A* 2012;**109**:2497−502.
32. Kim SH, Henry EC, Kim DK, Kim YH, Shin KJ, Han MS, et al. Novel compound 2-methyl-2*H*-pyrazole-3-carboxylic acid (2-methyl-4-*o*-tolylazo-phenyl)-amide (CH-223191) prevents 2,3,7,8-TCDD-induced toxicity by antagonizing the aryl hydrocarbon receptor. *Mol Pharmacol* 2006;**69**:1871−8.
33. Alahdal M, Xing Y, Tang T, Liang J. 1-Methyl-D-tryptophan reduces tumor $CD133^+$ cells, Wnt/β-catenin and NF-κβp65 while enhances lymphocytes NF-κβ2, STAT3, and STAT4 pathways in murine pancreatic adenocarcinoma. *Sci Rep* 2018;**8**:9869.
34. Li K, Wei L, Huang Y, Wu Y, Su M, Pang X, et al. Leptin promotes breast cancer cell migration and invasion *via* IL-18 expression and secretion. *Int J Oncol* 2016;**48**:2479−87.
35. Chen CH, Lu HI, Wang YM, Chen YH, Lo CM, Huang WT, et al. Areca nut is associated with younger age of diagnosis, poor chemoradiotherapy response, and shorter overall survival in esophageal squamous cell carcinoma. *PLoS One* 2017;**12**:e0172752.
36. Li Y, Huang B, Jiang X, Chen W, Zhang J, Wei Y, et al. Mucosal-associated invariant T cells improve nonalcoholic fatty liver disease through regulating macrophage polarization. *Front Immunol* 2018;**9**:1994.
37. Pham QT, Oue N, Sekino Y, Yamamoto Y, Shigematsu Y, Sakamoto N, et al. TDO2 overexpression is associated with cancer stem cells and poor prognosis in esophageal squamous cell carcinoma. *Oncology* 2018;**95**:297−308.
38. Ochs K, Ott M, Rauschenbach KJ, Deumelandt K, Sahm F, Opitz CA, et al. Tryptophan-2,3-dioxygenase is regulated by prostaglandin E2 in malignant glioma *via* a positive signaling loop involving prostaglandin E receptor-4. *J Neurochem* 2016;**136**:1142−54.
39. Whiteside TL, Demaria S, Rodriguez-Ruiz ME, Zarour HM, Melero I. Emerging opportunities and challenges in cancer immunotherapy. *Clin Cancer Res* 2016;**22**:1845−55.
40. Takenaka MC, Gabriely G, Rothhammer V, Mascanfroni ID, Wheeler MA, Chao CC, et al. Control of tumor-associated macrophages and T cells in glioblastoma *via* AHR and CD39. *Nat Neurosci* 2019;**22**:729−40.
41. Xiao P, Long X, Zhang L, Ye Y, Guo J, Liu P, et al. Neurotensin/IL-8 pathway orchestrates local inflammatory response and tumor invasion

by inducing M2 polarization of tumor-associated macrophages and epithelial−mesenchymal transition of hepatocellular carcinoma cells. *Oncoimmunology* 2018;**7**:e1440166.
42. Bishnupuri KS, Alvarado DM, Khouri AN, Shabsovich M, Chen B, Dieckgraefe BK, et al. IDO1 and kynurenine pathway metabolites activate PI3K−Akt signaling in the neoplastic colon epithelium to promote cancer cell proliferation and inhibit apoptosis. *Cancer Res* 2019;**79**:1138−50.
43. Li P, Chen X, Qin G, Yue D, Zhang Z, Ping Y, et al. Maelstrom directs myeloid-derived suppressor cells to promote esophageal squamous cell carcinoma progression *via* activation of the Akt1/RelA/IL8 signaling pathway. *Cancer Immunol Res* 2018;**6**:1246−59.
44. Fox Emily M, Gabriela Kuba María, Miller Todd W, Davies Barry R, Arteaga Carlos L. Autocrine IGF-I/insulin receptor axis compensates for inhibition of AKT in ER-positive breast cancer cells with resistance to estrogen deprivation. *Breast Cancer Res* 2013;**15**:R55.
45. Wei WQ, Chen ZF, He YT, Feng H, Hou J, Lin DM, et al. Long-term follow-up of a community assignment, one-time endoscopic screening study of esophageal cancer in China. *J Clin Oncol* 2015;**33**:1951−7.
46. Chen W, Zheng R, Baade PD, Zhang S, Zeng H, Bray F, et al. Cancer statistics in China, 2015. *CA Cancer J Clin* 2016;**66**:115−32.
47. Pyonteck SM, Akkari L, Schuhmacher AJ, Bowman RL, Sevenich L, Quail DF, et al. CSF-1R inhibition alters macrophage polarization and blocks glioma progression. *Nat Med* 2013;**19**:1264−72.
48. Colegio OR, Chu NQ, Szabo AL, Chu T, Rhebergen AM, Jairam V, et al. Functional polarization of tumour-associated macrophages by tumour-derived lactic acid. *Nature* 2014;**513**:559−63.
49. Condeelis J, Pollard JW. Macrophages: obligate partners for tumor cell migration, invasion, and metastasis. *Cell* 2006;**124**:263−6.
50. Franklin RA, Liao W, Sarkar A, Kim MV, Bivona MR, Liu K, et al. The cellular and molecular origin of tumor-associated macrophages. *Science* 2014;**344**:921−5.
51. Thaker AI, Rao MS, Bishnupuri KS, Kerr TA, Foster L, Marinshaw JM, et al. IDO1 metabolites activate β-catenin signaling to promote cancer cell proliferation and colon tumorigenesis in mice. *Gastroenterology* 2013;**145**:416−25.e1-4.
52. Cheong JE, Sun L. Targeting the IDO1/TDO2-KYN-AhR pathway for cancer immunotherapy—challenges and opportunities. *Trends Pharmacol Sci* 2018;**39**:307−25.
53. Lob S, Konigsrainer A, Rammensee HG, Opelz G, Terness P. Inhibitors of indoleamine-2,3-dioxygenase for cancer therapy: can we see the wood for the trees?. *Nat Rev Cancer* 2009;**9**:445−52.
54. Zhang J, Li H, Wu Q, Chen Y, Deng Y, Yang Z, et al. Tumoral NOX4 recruits M2 tumor-associated macrophages *via* ROS/PI3K signaling-dependent various cytokine production to promote NSCLC growth. *Redox Biol* 2019;**22**:101116.
55. Valeta-Magara A, Gadi A, Volta V, Walters B, Arju R, Giashuddin S, et al. Inflammatory breast cancer promotes development of M2 tumor-associated macrophages and cancer mesenchymal cells through a complex chemokine network. *Cancer Res* 2019;**79**:3360−71.
56. Guicciardi ME, Trussoni CE, Krishnan A, Bronk SF, Lorenzo Pisarello MJ, O'Hara SP, et al. Macrophages contribute to the pathogenesis of sclerosing cholangitis in mice. *J Hepatol* 2018;**69**:676−86.